

Heavy-quark and lepton-pair production on nuclei

K. Borekov,* A. Capella, A. Kaidalov,* and J. Tran Thanh Van

Laboratoire de Physique Théorique et Hautes Energies, Université de Paris XI, Bâtiment 211, 91405 Orsay CEDEX, France

(Received 12 February 1992)

We present a description of the A dependence of heavy-quark and Drell-Yan pair production in hadron-nucleus collisions, based on the Reggeon approach to strong interactions at high energies and the parton model. The same method has been successfully applied to the production of light-quark states. The existence of a new energy scale, which depends on the mass and x_F of the heavy system, is emphasized. A phenomenological model, which includes both the shadowing corrections to the nucleon structure function and the rescattering of the heavy-quark states, is proposed. The model quantitatively describes the available experimental data on J/ψ and heavy lepton-pair production in hA collisions as well as the European Muon Collaboration effect at low x .

PACS number(s): 24.85.+p, 12.40.Gg, 25.40.Ve, 25.80.Ls

I. INTRODUCTION

Investigation of hadronic interactions with nuclei at high energies can give important information on the space-time picture of strong interactions. To understand the A dependence of particle production both for hadrons made out of light (u, d, s) quarks and of heavy (c, b) quarks is a challenge for theoretical models of high-energy interactions.

There is a general approach to hadronic interactions at high energies [1] based on Reggeon field theory and the parton model. For collisions involving nuclei this framework is also known as the Glauber-Gribov model [2,3]. Particular, QCD-based, realizations of this general approach are the dual parton model (DPM) [4] and the quark gluon string model (QGSM) [5], which successfully describe multiparticle production in hadronic and nuclear collisions. We will use this general formalism to study the A dependence of heavy-quark and lepton-pair production. Application of this framework for "hard" processes is justified, because we are interested in the soft rescatterings in nuclei, which accompany hard interactions (shadowing effects).

An important tool for analysis of multiparticle processes is provided by the celebrated Abramovskii, Gribov, Kancheli (AGK) rules [6]. These rules give relations between various multiparticle discontinuities (cuttings) of an elastic amplitude and result in remarkable cancellations of different contributions in some physical quantities. One of the best known of AGK cancellations is in single-particle inclusive spectra. Here the various cuttings of the dominant, nonenhanced diagrams,¹ cancel with each other and, as a result, only the single-Reggeon term survives giving an A^1 behavior.

However, there is a number of effects violating AGK rules [7–9]. The AGK rules are applicable only to particles emitted from cut reggeon propagators. If the emitted particles belongs to the upper "blob" of the diagram, the AGK cancellation is not valid.

The most obvious physical mechanism of AGK-rule violation is related to energy-momentum conservation [7]. The sharing of the available energy among the various inelastic collisions (or the various strings) causes the x_F distribution for the cuttings of several Reggeons to be softer than the one for the single-Reggeon cutting.

The experimentally observed variety of A behaviors for different particles in different x_F regions gives evidence for AGK-rule violations.

Let us consider first the production of light-quark states. Experimentally the A dependence for ordinary hadrons ($\pi, K, N, \Lambda, \dots$) parametrized as A^α is as follows (for a review see Ref. [10]): α is slightly larger than one in the nucleus fragmentation region and decreases steadily to a value $\alpha \approx 0.4$ – 0.5 in the projectile fragmentation region. These data are naturally described as a result of momentum conservation [4,5]. The value $\alpha \sim 0.4$ – 0.5 at $x_F \sim 1$ is an edge effect associated to a large interaction cross section of the light-quark hadron ($\sigma \sim 20$ – 30 mb). (See Sec. III.)

For heavy-quark states and Drell-Yan (DY) lepton pairs the situation is quite different. Experimentally $\alpha \approx 1$ for Drell-Yan process, except at the highest available energies (800 GeV/c) and for large x_F , where $\alpha \approx 0.95$ [11]. For J/ψ , $\alpha \approx 0.9$ at $x_F \sim 0$ and decreases to $\alpha \approx 0.7$ – 0.8 at $x_F \sim 1$ [11,12]. A value of $\alpha < 1$ has also been observed for ψ' and Υ production [11]. These results are difficult to explain in most available models [13]. We will show that they can be explained in our approach.

The shadowing for heavy-state production can be caused by rescattering both of light-quark hadrons accompanying the heavy state and of this state itself. (The latter interaction is absent for Drell-Yan process.) The key point is the existence of an energy scale E_M , where AGK rules break due to t_{\min} effects [8]. Below this critical energy the cuttings associated to coherent diffractive

*Also at ITEP, 117259 Moscow, USSR.

¹Nonenhanced diagrams are diagrams without Reggeon interaction as in Fig. 1. Enhanced diagrams contain Reggeon interaction.

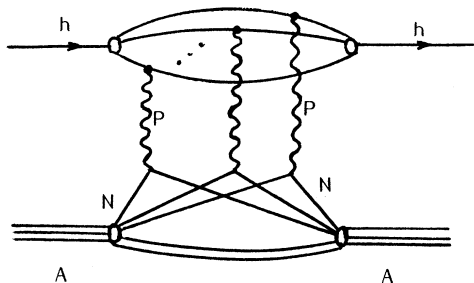


FIG. 1. Nonplanar Reggeon diagram for hadron-nucleus scattering.

production on nucleus vanish and the A dependence can drastically change when this critical scale is crossed. The important role of this new large-energy scale for heavy-state production was stressed in Ref. [9], where the qualitative features of this approach have been discussed. The value of this critical energy (which depends on the mass M , the x_F of the produced particle and also on the nuclear size R_A) is of order $E_M \sim M^2 R_A$ (see Sec. II for details).

There is also another critical scale E_0 , where the interplay of nonplanar (Fig. 1) and planar (Fig. 2) graphs is essential [14,3,8]. The space-time picture of the interaction changes at this scale crucially. However, the elastic amplitude [3] and all its discontinuities corresponding to multiple-Reggeon cuttings behave smoothly [8].

For light-quark hadron production this scale coincides with the t_{\min} scale and equals $E_0 \sim m_N \mu R_A$, where μ is a typical mass scale of strong interactions.

For heavy-state production, the scales E_0 and E_M are different and there is a large region $E_0 < E < E_M$ where the shadowing effects for Drell-Yan process are canceled. For the latter, the shadowing at high energies $E > E_M$ is mainly due to nonplanar enhanced Reggeon graphs and the absorption at $E < E_0$ results from planar graphs.

As for the rescattering of the heavy state itself, this mechanism is just like the momentum-conservation effect for light hadrons but with a quantitative difference which is due to the fact that the heavy state carries after rescattering a large momentum fraction and, therefore, the effect is concentrated at larger x_F values. This mechanism is present both at $E < E_M$ and at $E > E_M$.

This paper is organized as follows: in Sec. II we review the parton-Reggeon approach (partonic version of the

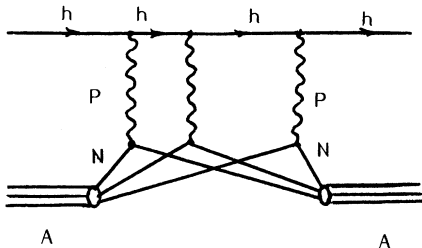


FIG. 2. Planar Reggeon diagram for hadron-nucleus scattering.

Glauber-Gribov model) and the existence of the critical energy scales E_0 and E_M . In Sec. III we apply this approach to the production of ordinary hadrons made out of light quarks. We give the results of the Feynman-diagram analysis for the A dependence, as well as the prescriptions to compute it. In Sec. IV we discuss lepton-pair production and show the almost complete cancellation of the shadowing corrections at present energies. In Sec. V we consider the production of heavy-quark states and show that the rescattering is important and leads to a decrease of α with increasing x_F . In Sec. VI we present a phenomenological realization of our approach. It takes into account the effects discussed in the previous sections combining the heavy-state interaction with the shadowing corrections due to light partons interaction. The effects of the energy scale E_M are included in our formulation. A comparison with available data on A dependence of nucleon structure functions and for Drell-Yan and J/ψ -production cross section is presented. In Sec. VII we compare our approach with other models, in particular with intrinsic-charm model. Section VIII contains our conclusions. Some technical aspects of the model of Sec. VI are given in Appendix A.

II. INTERACTION OF HADRONS WITH NUCLEI IN THE PARTON MODEL AND REGGE APPROACH

In this section we will review some general features of the approach based on the Gribov Reggeon calculus [1] in the case of hadron-nucleus interactions [3].

The fast moving hadron in this approach cannot be considered as a single particle passing through a nuclear medium, but as a superposition of different multiparticle states (Fock-state vector). It is usually assumed also that only states which have wee partons can effectively interact with a target. The states which contain only fast partons are sterile and do not interact. The lifetime of a fluctuation which contains wee partons is large and is proportional to the initial energy of the colliding hadron h ($\tau \sim E/\mu m_h$, where μ is a characteristic scale of strong interaction). So this fluctuation starts to develop long before the interaction of its wee partons with the target takes place. The interaction of these soft partons with the target destroys the coherence of the state, and the virtual inelastic state starts to transform into a real hadronic state. Because of unitarity this inelastic interaction leads also to elastic scattering, which corresponds to Pomeron exchange.

Each component of the fluctuation can produce its own wee partons and an interaction of several independent pieces of the fluctuation leads to Regge cuts in the hA elastic amplitude and is described by the nonplanar (Mandelstam-type) diagrams of Fig. 1. These fluctuations develop simultaneously and thus at high energies it is impossible to speak of successive rescatterings of the initial hadron.² So the fast hadron colliding with a nucleus can

²The planar diagrams which correspond to successive rescatterings of the initial particle are important for $E < E_0$ and decrease as $1/E$ for $E > E_0$ [3,14].

be viewed as a complicated multiparticle system with several soft components, which can interact with different nucleons of a nucleus—inside a tube with a given impact parameter of the hadronic size. The interaction of such a system, which slightly reminds of an “octopus,” with a nucleus is shown schematically in Fig. 3. Interactions of each “tentacle” can have either inelastic or absorptive character and correspond to various cuttings of the Reggeon diagrams for the elastic hA amplitude (Fig. 1). The relations between the contributions of these cuttings can be obtained from an analysis of the corresponding discontinuities of the Reggeon diagrams. They are different for asymptotic energies $E > E_0$ (AGK cutting rules) and for energies $E < E_0$ [8].

Although the space-time picture of interaction at high energies $E > E_0$ is completely different from the Glauber one, the generalized Glauber-type formula for the elastic hA scattering amplitude, which takes into account inelastic diffractive production, is valid [3].

The diagrams of Fig. 1 start to dominate in the energy region $E \geq E_0$, where the diffractive production with small momentum transfer $|t| \sim 1/R_A^2$ to nucleons ($R_A \approx R_0 A^{1/3}$ is the radius of the nucleus) becomes possible (Fig. 4). The critical energy E_0 can be determined from the condition on the minimal invariant momentum transfer $|t_{\min}| \sim 3/R_A^2$. [The t dependence of the form factor of a nucleus $F(t)$, which enters the diagram of Fig. 1, is parametrized in the form $F(t) = \exp(R_A^2 t/6)$.] More precisely,

$$t_{\min} \approx \frac{(\bar{s}_1 - m_h^2)^2}{4E_0^2} \sim \frac{3}{R_A^2}, \quad (1)$$

where \bar{s}_1 is the mean mass square of the diffractively produced system. For “ordinary” hadrons (made of light u, d, s quarks and gluons) $\bar{s}_1 - m_h^2 \approx (1-2) \text{ GeV}^2$ and $E_0 \sim (5-10) \text{ GeV}$.

For energies lower than the critical energy E_0 the longitudinal size (time) of the fluctuation is less than the size of a nucleus and it is possible to speak of *successive* re-

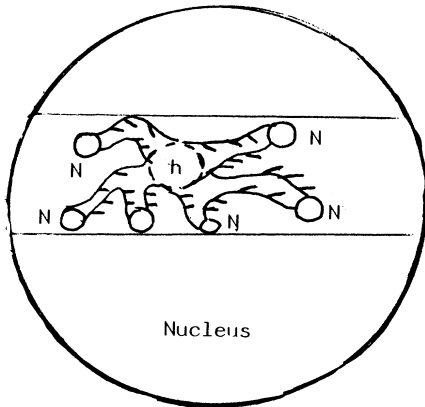


FIG. 3. Interaction of different components of a fluctuation of the incoming hadron wave function with different nucleons of the nucleus.

scatterings of an initial hadron on different nucleons of a nucleus. In this energy region a coherent diffraction dissociation process is impossible—it is damped by the nuclear form factor. However, at energies $E > E_0$ the picture of *simultaneous* interaction of the initial fluctuation with different nucleons of the nuclei described above becomes valid.

For production of systems containing heavy quarks Q (c, b) or lepton pairs with large mass M the critical energy at which the space-time picture of the interaction with nuclei changes is much larger. Consider as an example the production of a $Q\bar{Q}$ system ($J/\psi, \chi, \Upsilon, \dots$) with mass M ($M/\sqrt{s} \ll 1$). We will show in Sec. III that the nontrivial nuclear effects (difference from A^1 for inclusive spectra) are associated only with the diagrams where the heavy quarks belong to the partonic fluctuation of the initial hadron (the upper blob in Fig. 1). These diagrams are nonzero only at energies where the corresponding heavy system can be produced coherently in the diffractive process (Figs. 4 and 5). Thus in this case (for $h=N$) $s_1 \geq (M + m_N)^2$ and

$$E_M \geq (M^2 + 2Mm_N)R_A/2\sqrt{3}, \quad (2)$$

which for $A^{1/3} \approx 4$ is equal to 100–200 GeV for J/ψ and $\sim 10^3$ GeV for Υ .

It should also be taken into account that the mass of the hadronic system which is produced together with $Q\bar{Q}$ (or l^+l^-) is substantially higher than m_N and increases as x_F of the $Q\bar{Q}$ decreases. In order to obtain a more realistic estimate of the value of \bar{s}_1 let us consider the diffractive production of a heavy-quark system $Q\bar{Q}$ shown in Fig. 5(a). Then, taking into account that $M^2 \approx sx_1x_2$, $x_F = x_1 - x_2$ (where x_1 is the fraction of the momentum of the initial hadron carried by the gluonic system which produces a $Q\bar{Q}$ pair, and x_2 is the momentum fraction of the second nucleon carried by the Pomeron P) we obtain

$$x_1 = x_+, \quad x_2 = x_-,$$

where $x_{\pm} = \frac{1}{2}(\sqrt{x_F^2 + 4M^2/s} \pm x_F)$ and therefore $\bar{s}_1 = x_2s = M^2/x_+$.

The value of \bar{s}_1 increases as x_F decreases and $\bar{s}_1 = M\sqrt{s}$ for $x_F = 0$. In the following we will often use the variables x_{\pm} which are simply related to the rapidity of the heavy state $x_{\pm} = M/\sqrt{s} \exp(\pm y)$. A completely analogous result is obtained for the diffractive mechanism shown in Fig. 5(b).

Thus the critical energy for the production of states

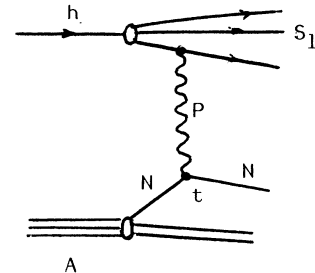


FIG. 4. Diffractive production of a hadronic system.

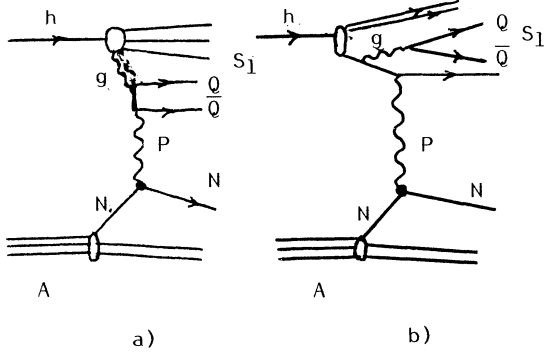


FIG. 5. Diffractive production of a hadronic system accompanied of a $Q\bar{Q}$ pair.

with large masses is

$$E_M = \frac{M^2 R_A}{2x_+ \sqrt{3}}. \quad (3)$$

The values of E_M for J/ψ , Υ and lepton-pair production with $M=5$ GeV for different x_F (and $A \sim 100$) are given in Table I.

It follows from these estimates that for J/ψ the change of regime occurs in the presently accessible range of energies, while for Υ this will happen at higher energies.

III. PRODUCTION OF THE LIGHT-QUARK STATES

The Reggeon diagram technique [1,3] allows to calculate the contributions of Reggeon diagrams of Fig. 1 to the elastic hA amplitude and to the cross section of particle production.³ In the approximation in which inelastic diffraction dissociation is neglected, these expressions coincide with the standard Glauber formulas

$$\sigma_{hA}^{(\text{tot})} = 2 \int d^2b \left[1 - \exp \left[-\frac{\sigma_{hN}^{(\text{tot})}}{2} n_A(b) \right] \right], \quad (4)$$

$$\sigma_{hA}^{(\text{prod})} = \int d^2b \{ 1 - \exp[-\sigma_{hN}^{(\text{in})} n_A(b)] \}, \quad (5)$$

where $n_A(b)$ is a nuclear profile function in the impact parameter space [$\int d^2b n_A(b) = A$]. In this approach, using the AGK cutting rules, it is also possible to calculate contributions of diagrams with fixed number of cut Pomerons k and an arbitrary number of uncut ones (absorption). Using the same approximation that leads to Eqs. (4) and (5), one has

$$\sigma_k^{hA}(b) = \frac{[\sigma_{hN}^{(\text{in})} n_A(b)]^k}{k!} \exp[-\sigma_{hN}^{(\text{in})} n_A(b)]. \quad (6)$$

Although these formulas are sometimes interpreted in the

³Note that this technique allows one to work in hA scattering not with Reggeons (Pomerons) but with the full hN amplitudes. In the following we will use the term Pomeron instead of hN amplitude for simplicity.

TABLE I. Values of E_M (in GeV) for J/ψ , Drell-Yan ($M=5$ GeV) and Υ for different values of x .

	$x=0$	$x=0.2$	$x=1$
J/ψ	10^3	280	70
DY ($M=5$ GeV)	2.5×10^3	700	170
Υ	10^4	2.5×10^3	650

framework of a naive probabilistic picture as successive interactions of the initial hadron, it should be kept in mind that at high energies the physical mechanism of interaction is quite different as it was emphasized in Sec. II.

The A dependence of the inclusive cross section is as follows. For a particle a , emitted from a cut Pomeron, one has

$$f_{hA}^a \equiv E \frac{d^3 \sigma_{hA}^a}{d^3 p} \propto \sum_{k=1}^{\infty} k \sigma_k = A \sigma_{hN}^{(\text{in})} \quad (7)$$

(the factor k reflects the fact that for k cut Pomerons the particle a can be emitted from any of them).

This result, which is trivial in the Glauber model, is quite general and can be proved for any set of Feynman diagrams of “nonenhanced” type (without interactions between Pomerons), Fig. 1.

The situation changes, however, if particle a comes from cutting the upper blob in Fig. 1. In this case the factor k in Eq. (7) is not present and if we neglect the absorption (final-state interaction) of a particle a the A dependence of the inclusive cross section is

$$f_{hA}^a \propto \sum_{k=1}^{\infty} \sigma_k = \sigma_{hA}^{(\text{in})} \propto A^{2/3}. \quad (8)$$

Moreover, if final-state interaction of the hadron a is possible, then $\alpha < \frac{2}{3}$ for $x_F \sim 1$ [see Eq. (10) and the discussion that follows it].

This results can be made more quantitative in the framework of the DPM and QGSM. The inclusive cross section of hadron a is written as a sum of contributions from different chains or strings:

$$f_{hA}^a = \sum_{k=1}^{\infty} k \sigma_k F_k^a(x_F, p_T^2, s). \quad (9)$$

In this expression the summation over an arbitrary number m of uncut Pomerons (which leads to absorption), was performed and it was assumed that these absorptive rescatterings do not affect the structure of the final state for a given number k of inelastic interactions. In other words, it was assumed that the corresponding functions $F_{k,m}^a(x_F, p_T^2, s)$ do not depend on m . An analysis of the Feynman diagrams supports this assumption (see below at the end of this section). This prescription allows one to take into account the effects due to momentum conservation and to study the A dependence of inclusive cross section as a function of x_F .

At large energies and small x_F the functions $F_k^a(x_F, p_T^2, s)$ do not depend on k and Eq. (7) is valid. However for $x_F \rightarrow 1$ the momentum-conservation effects become important. The energy of the initial hadron is shared between the various constituents at the string

ends. The mean energy per inelastic interactions decreases as their number k increases and the probability to produce a hadron with $x_F \rightarrow 1$ decreases also. Consider as an example $\sigma_{hN}^{(in)} F_k^a = f_{hN}^a(x_F, p_T^2)(1-x_F)^{k-1}$ (cf. Appendix A), then

$$f_{hA}^a = f_{hN}^{(a)} \int d^2b n_A(b) \exp[-\sigma_{hN}^{(in)} n_A(b) x_F]. \quad (10)$$

This expression for f_{hA}^a coincides with Eq. (7) as $x_F \rightarrow 0$ and it demonstrates the general rule—the strength of the absorption increases (and the value of α decreases) as $x_F \rightarrow 1$. For $x_F \rightarrow 1$ only F_1 survives and f_{hA}^a behaves as

$$\sigma_1^{hA} = \sigma_{hN}^{(in)} \int d^2b n_A(b) \exp[-\sigma_{hN}^{(in)} n_A(b)],$$

which for very large A gives $\alpha \approx \frac{1}{3}$ —only the edge of the nucleus contributes. In the DPM and QGSM the functions F_k are completely determined in terms of the momentum distributions and fragmentation functions of quarks (diquarks) in the colliding hadrons [4,5]. The example above just illustrates the qualitative features of DPM and QGSM. [The actual calculations show in fact that at $x_F=0$, $\alpha=1$ only asymptotically and at present energies the cross section in the exponent of Eq. (10) is multiplied by a term $\sim x_+ = m_T^a/\sqrt{s}$ (for $x_F=0$), which leads to $\alpha < 1$.] These models give a good, parameter-free description of experimental data on inclusive spectra of light hadrons (p, K, N, Λ, \dots) in hA collisions [4,5,28]. Thus momentum conservation effects lead to a definite pattern of violation of the AGK cancellation for inclusive spectra in DPM and QGSM.

The diagrammatic approach which is the starting point for a consistent derivation of the Glauber-type formulas allows us to study the validity of the prescription described above. To illustrate this point we discuss an example single and double rescattering diagrams. These diagrams and their one and two Pomeron cuttings are shown in Figs. 6 and 7. As it was pointed out above, there are two ways for producing particle a : the first is connected to cutting of Pomerons and the second is due to the presence of a in the “blob.”

In the first case, the negative contribution from the diagrams of Fig. 7(b) is exactly canceled by the positive contribution from the diagram of Fig. 7(c) (note that the particle a can be taken from both chains of this diagram). This result is valid for any kinematical configuration of final particles. Thus in this case the AGK cancellation is exact and is not influenced by momentum conservation. This is the derivation of Eq. (7) in terms of Reggeon diagrams.

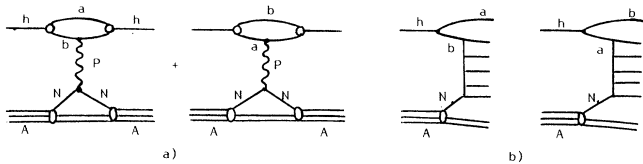


FIG. 6. (a) Single-Pomeron-exchange diagram and (b) its s -channel cut.

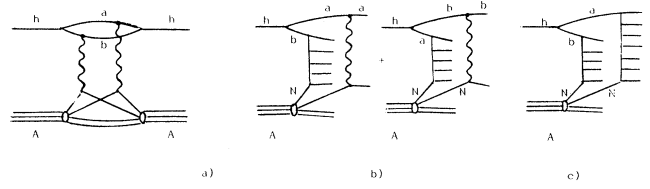


FIG. 7. (a) Double-Pomeron-exchange diagram and (b) its s -channel cuttings across one Pomeron and (c) two Pomerons.

On the contrary, when particle a is emitted from the “blob,” the AGK cancellation is no longer valid.⁴ This contribution is important mainly in the fragmentation region of the projectile and leads to a modification of the A^1 dependence due to absorption. Note that the absorption does not change the structure of the final state [compare Figs. 6(b) and 7(b)] justifying an assumption made in deriving Eq. (9). Note also that this absorption is determined by the cross section σ_{aN} of the produced particle with a nucleon and not by the cross section σ_{hN} of the initial hadron h , as in Eq. (9). Thus the usual prescription of Eq. (9) is justified only if the cross sections of all the “constituents” are approximately equal. This is true for particles made of light quarks (especially in DPM and QGSM, where the “constituents” are not some special hadrons but colorless pieces of strings with universal distribution of their ends). On the other hand, particles made of heavy quarks can have cross sections of interaction with nucleons substantially different from $\sigma_{\pi N}$ (or σ_{NN}) as well as different distributions functions, and the results of the diagrammatic approach have to be taken into account.

IV. DRELL-YAN PROCESS

It is a widely spread belief that a hard process should have an A^1 dependence. However, this conclusion cannot be universal as it is intuitively clear that for a macroscopic lump of matter the incident beam will be damped, so the process cannot proceed independently on all nucleons of the target [16]. At available energies the experimental data on Drell-Yan process demonstrate the A^1 behavior with a good accuracy. So in our approach we should understand this behavior and determine the regions where the A^1 dependence breaks.

To proceed let us summarize the conclusions of the previous section. For the production of an arbitrary particle a there are two different contributions.

(i) If the particle a is emitted from a cut Pomeron, the inclusive cross section behaves as A^1 . More precisely, contributions to the inclusive cross section due to cutting of Pomerons in Fig. 1 always cancel for any number of exchanged Pomerons $n \geq 2$. The single interaction diagram $n=1$ [Fig. 8(a)] leads to the A^1 behavior.

(ii) If the particle a is produced in the upper “blob” [Fig. 8(b)], the A^1 behavior is no longer true, and the A dependence is influenced in general by the value of the cross section σ_{aN} .

⁴This problem has been studied in detail by Braun [15].

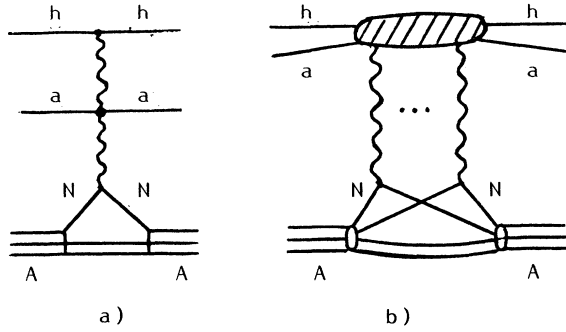


FIG. 8. Inclusive production of a particle a emitted (a) from a Pomeron propagator and (b) from the upper blob.

In the case of heavy lepton-pair production the system $a = l^+ l^-$ does not interact strongly with nucleons. On the other hand, other partons in the initial configuration can interact with different nucleons of a nucleus (Fig. 9) and lead to a modification of the A^1 dependence. However a heavy fluctuation with mass $\sqrt{s_1} > M_{l^+ l^-}$ can lead to nonzero rescattering effects in nucleus only for large enough energies, as it was explained in Sec. II. According to Eq. (3) the critical energy is

$$s_M = 2m_N E_M = \frac{M^2}{x_+} \frac{m_N R_A}{\sqrt{3}}. \quad (11)$$

For fixed energy few can introduce the critical values of x_+ and y :

$$x_+^{\text{crit}} = \frac{M}{\sqrt{s}} \exp(y^{\text{crit}}) = \frac{M^2}{2E} \frac{R_A}{\sqrt{3}}. \quad (12)$$

For energies $E < E_M$ the contribution of the rescattering diagrams of Fig. 9 is zero and an A^1 dependence is obtained. Let us note that some of the cuttings of this diagram are not zero, but they are modified from the AGK values due to the same t_{\min} effect [8]. For example for a two-Pomeron-exchange diagram the coefficients for cuttings corresponding to diffraction dissociation, absorption (cutting of one Pomeron) and cutting of two Pomerons change from $+1$, -4 , $+2$ at $E > E_M$ to 0 , -2 , $+2$ at $E < E_M$. The sum of all contributions at low energies is zero as it should be. Physically this result is due to the fact that for $E < E_M$ the coherence length of the fluctuation is smaller than the size of the nucleus and the longitudinal ordering of nucleons becomes important.

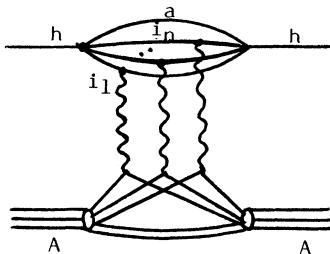


FIG. 9. Nonplanar diagram for the case when a constituent a of the upper blob does not interact with nucleons.

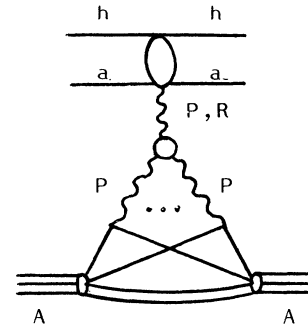


FIG. 10. Enhanced diagram for the inclusive production of particle a .

Triggering on the lepton pair does not modify the relations between different cuttings, so the inclusive cross section for heavy lepton-pair production for $E < E_M$ is not influenced by the rescattering effects and behaves as A^1 .

In the perturbative QCD formulation, where $l^+ l^-$ production is due to $q\bar{q}$ annihilation, the value of x_2 [momentum fraction of a quark (antiquark) from a nucleus] is given by $x_2 = x_- = M^2/sx_+$. So the condition $s > s_M$ for the existence of rescattering effects corresponds in this language to the condition

$$x_x < x_{2A}^{\text{crit}} \equiv \frac{\sqrt{3}}{m_N R_A}, \quad (13)$$

which is well known from the studies of screening effects in the structure functions of nuclei [17–19]. Thus for heavy lepton-pair production an A dependence different from A^1 can be obtained only for very small values of x_2 .⁵

Let us consider the interaction of soft partons in the initial configuration, with nucleons of the target. The interaction of these soft partons corresponds to the Reggeon diagram shown in Fig. 10. (Graphs of the eikonal type are not present here since the DY pair does not interact and therefore the pole contribution is not present. Thus the absorptive corrections to lepton-pair production are expected to be small even at $E > E_M$.) The diagram of Fig. 10 with only the P pole contribution factorizes and leads to an A dependence of inclusive cross section which can be absorbed into a function of only one variable $x_2 = M^2/sx_+$. The same function describes the small- x dependence of structure functions of nuclei as measured in deep inelastic scattering (Fig. 11). So this contribution to the Drell-Yan process is in agreement with the factorization theorem proved in perturbative QCD [20]. However, in principle, there can be nonfactorizable pieces for example due to secondary-Reggeon (R) contributions in the diagram in Fig. 10.

The result obtained above for the factorizable piece is consistent with the standard theoretical interpretation of

⁵We do not discuss here the modification of the nuclear structure function at large $x_2 \geq 0.2$ due to non-nucleonic degrees of freedom.

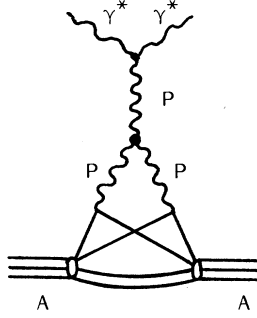


FIG. 11. Triple-Pomeron diagram for the nucleon structure function at small x .

hard processes on nuclei, where the difference of the A dependence of nuclear structure functions from A^1 in the region of small x is attributed to the shadowing of partons belonging to different nucleons of a nucleus. Note that the same effect can be considered as a result of rescatterings of soft partons of the initial partonic fluctuation on different nucleons of a nucleus. The first interpretation is relevant in the system where a nucleus has a large momentum, while the second one is more natural in the rest system of a nucleus. So one should not take into account both effects simultaneously to avoid potential double counting. This problem is avoided with the use of the Reggeon diagram technique.

To conclude this section we discuss an interesting question posed at its beginning: what are the distances where the classical picture of the beam absorption in matter is restored? For this purpose let us consider the Drell-Yan process at very large fixed energy as a function of the longitudinal distance r between nucleons of the target. At distances $r < r_M \simeq 2Ex_+/M^2$ there will be the shadowing discussed above and the A dependence is different from A^1 ($\alpha < 1$). When $r_M < r < r_0 \simeq E/m\mu$ only nonplanar diagrams are important, but the shadowing is absent, and the inclusive cross section behaves as A^1 . The new regime takes place at extremely large values of $r > r_0$. In this region the planar diagrams of the type shown in Fig. 2 become important, while all nonplanar diagrams (even with light-quark states in the blob) are zero. It follows from the analysis of diagrams that in this region a simple classical probabilistic picture of successive interactions of the initial hadron is restored [8]. Thus for this large distances an "absorption of the beam" takes place.

V. PRODUCTION OF HEAVY-QUARK STATES

An essential difference between the production of lepton pairs and heavy-quark $Q\bar{Q}$ states ($J/\psi, \psi', \chi, \Upsilon, \Upsilon', \dots$) is that in the latter case strong interaction with nucleons is possible.

Consider a fluctuation of the initial hadron containing a pair $Q\bar{Q}$ and a number of ordinary light quarks. There are two types of interaction of this fluctuation with target nucleons. The first one is an interaction of light-quark hadrons, which accompany the heavy-quark system. This interaction is of the same type as in Drell-Yan case and was discussed in the previous section. It reminds of

the "intrinsic charm" mechanism with the difference that, according to Regge dynamics, it starts to work only at energies large enough, $E > E_M$ (see also Sec. VII).

In this section we will be interested in the interaction of the second type, when the heavy-quark state interacts with the nucleus.

We can imagine two different mechanisms for this interaction depending on the color state of the pair. If $Q\bar{Q}$ is produced in a colorless state the value of the interaction cross section presumably decreases with the mass of the heavy quark. This colorless system has a long formation time [13] of order of $E/M\mu$, where M is its mass. (Because of the Chudakov effect this system interacts as a dipole.) On the other hand, if this system interacts, it is easily absorbed transforming into mesons with open heavy flavor. (B) The $Q\bar{Q}$ pair is produced in a color state and is accompanied by light quarks in order to make the system colorless. This mechanism is natural in DPM and QGSM if string breaks due to $Q\bar{Q}$ -pair creation. In this case a pair of heavy hadrons is produced (for example, $D\bar{D}, B\bar{B}, \dots$). We will denote this colorless system of heavy and light quarks as " $Q\bar{Q}$ " for short. This system goes through the nucleus interacting with a comparatively large cross section due to the presence of light quarks. As a consequence the difference between light- and heavy-quark systems regarding their interaction cross section (see the discussion at the end of Sec. III) turns out to be rather unessential. The interactions of the " $Q\bar{Q}$ " system can be both elastic and inelastic. After inelastic interaction the " $Q\bar{Q}$ " system loses a part of its momentum due to extra particle production. With some small probability the " $Q\bar{Q}$ " system can transform into a colorless $Q\bar{Q}$ system ($J/\psi, \Upsilon$) plus light hadrons.

In this paper we will concentrate on mechanism (B) suggesting that it is the dominant one. Let us discuss the main properties of this mechanism, limiting for simplicity the discussion to the case of single rescattering. More general formulas will be used in Sec. VI. The diagrams corresponding to the elastic and inelastic rescatterings are shown in Fig. 12. For Fig. 12(a) the " $Q\bar{Q}$ " momentum distribution is the same as for the diagram without rescatterings, i.e., $F_1(x_F)$. For Fig. 12(b) with inelastic rescattering the momentum distribution $F_2(x_F)$ is softer than $F_1(x_F)$ due to production of extra particles. If we denote the probability for the system " $Q\bar{Q}$ " to have a fraction z of the initial " $Q\bar{Q}$ " momentum after inelastic rescattering as $G^{Q\bar{Q}}(z)$, then

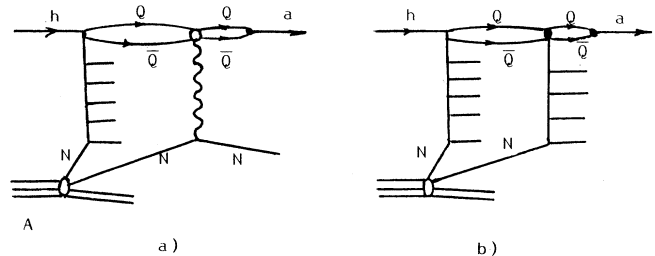


FIG. 12. (a) Elastic and (b) inelastic rescattering of a $Q\bar{Q}$ system. The latter does not have to be the leading one.

$$F_2^{Q\bar{Q}} = F_1^{Q\bar{Q}} \otimes G^{Q\bar{Q}}, \quad (14)$$

where the sign \otimes means a convolution operation (see the Appendix A for details). To obtain the momentum distribution of a final particle a the functions $F_1^{Q\bar{Q}}, F_2^{Q\bar{Q}}$ must be convoluted with some new function $G^a(z)$, determining the probability for “ $Q\bar{Q}$ ” to go into particle a :

$$F_i^a = F_i^{Q\bar{Q}} \otimes G^a, \quad i = 1, 2. \quad (15)$$

If functions F_1^a and F_2^a were identical the AGK cancellation would be valid, leading to an A^1 dependence. Because the function F_2^a decreases faster than F_1^a as $x_F \rightarrow 1$, absorptive corrections are present.⁶ This is exactly the same effect discussed in Sec. III for light quarks. The only quantitative difference between the two cases resides in the mass of the quark Q . The “ $Q\bar{Q}$ ” system produced in the second interaction (Fig. 12) carries a larger fraction of the primary-“ $Q\bar{Q}$ ” momentum than for light-quark systems and thus the difference between $F_1^a(x_F)$ and $F_2^a(x_F)$ will be concentrated in a region of x_F closer to unity as the mass of the “ $Q\bar{Q}$ ” system increases.

Another source of absorptive corrections within mechanism (B) is that, generally speaking, the projection of the “ $Q\bar{Q}$ ” state on the wave function of particle a can be different for diagrams with different number of rescatterings. In the phenomenological model of Sec. VI we will take into account this effect by introducing an additional parameter ϵ . Note that this parameter can also account for a possible absorption resulting from mechanism (A). Thus the interesting problem arises of separating these two mechanisms.

In conclusion, the main result of this section is that the absorption due to “ $Q\bar{Q}$ ” interaction persists even at energies $E < E_M$ and increases with x_F .

VI. THE PHENOMENOLOGICAL MODEL AND DESCRIPTION OF EXPERIMENT

Now we can construct a phenomenological model, which takes into account the theoretical ideas of the previous sections. Let us consider first Drell-Yan pair production.

Interactions of the soft partons of the type shown in Fig. 9 lead to an inclusive cross section of the noninteracting system described by the enhanced diagram of Fig. 10. We take them into account using the Schwimmer formula [21], which gives the result of summing all

⁶This difference between the functions F_1^a and F_2^a is responsible of the fact that, contrary to DY production, the t_{\min} effect does not cancel the absorptive corrections at $E < E_M$. Indeed from the discussion in Sec. IV [just below Eq. (12)] we see that, for DY production, the cancellation of the absorptive corrections at $E < E_M$ is due to the AGK weights of the single and double Pomeron cuttings (respectively -2 and $+2$). For heavy-flavor production the contribution of the first cutting is multiplied by $F_1^a(x_F)$ and that of the second one by $F_2^a(x_F)$ thereby preventing the cancellation at $E < E_M$.

diagrams with multiple triple-Pomeron interactions.⁷ At high energies $E > E_M$ the inclusive cross section due to this contribution has the form

$$f_{hA}^a(x_F, p_T^2) = f_{hN}^a(x_F, p_T^2) \int d^2b \frac{n_A(b)}{1 + n_A(b)C(x_+)}, \quad (16)$$

where the function $C(x_+)$ comes from rapidity integration

$$C(x_+) = g(y - y^{\text{crit}}) = g \ln(x_+ / x_+^{\text{crit}}), \quad (17)$$

or, in terms of the Bjorken variable x_2 ,

$$C = g \ln(x_{2A}^{\text{crit}} / x_2).$$

Here x_+^{crit} and y^{crit} are determined by Eq. (12) and x_{2A}^{crit} by Eq. (13).

The constant g is connected to the value of the triple-Pomeron coupling $r_{PPP}(0)$:

$$g = 2\pi r_{PPP}(0)g_N(0), \quad (18)$$

where $g_N(0)$ is the Pomeron-nucleon coupling at $t=0$. The value of r_{PPP} can be determined from the study of the high-mass diffractive production (see, e.g., Ref. [22]). We take also into account the PPR -term contribution by increasing somewhat the value of the constant g ($g \approx 1$ mb).

At energies $E \leq E_M$ the double rescattering graph of Fig. 10 is damped by a factor

$$\Phi \equiv \exp(R_A^2 t_{\min} / 3) = \exp[-(x_+^{\text{crit}} / x_+)^2]$$

(with $R_A = (0.82 A^{1/3} + 0.58)$ fm [23]). For high energies this factor is close to unity. So to generalize Eq. (16) to all values of E we write

$$f_{hA}^a(x_F, p_T^2) = f_{hN}^a(x_F, p_T^2) \int d^2b \frac{n_A(b)}{1 + n_A(b)\tilde{C}(x_+)\Phi}, \quad (19)$$

where⁸

$$\tilde{C}(x_+) = g \ln(1 + x_{2A}^{\text{crit}} / x_2).$$

For subcritical energies $E < E_M$, where $\Phi \ll 1$, we have an A^1 behavior,

$$f_{hA}^a(x_F, p_T^2) = A f_{hN}^a(x_F, p_T^2),$$

⁷We suggest, of course, as everywhere above, that not Pomerons but full hN amplitudes enter the Schwimmer formula in the spirit of Ref. [8]. Multi-“Pomeron” couplings have the meaning of effective ones. To simplify the model we retain only triple-Pomeron vertices neglecting quartic and higher couplings. With these approximation the formulae of Ref. [8] are equivalent to Eq. (16).

⁸In the absence of the form factor Φ the rapidity integration leads to Eq. (17). The modification of the function $C(x_F)$ takes into account, in an approximate way, the effect of the form factor in the rapidity integration and ensures the positivity of this function.

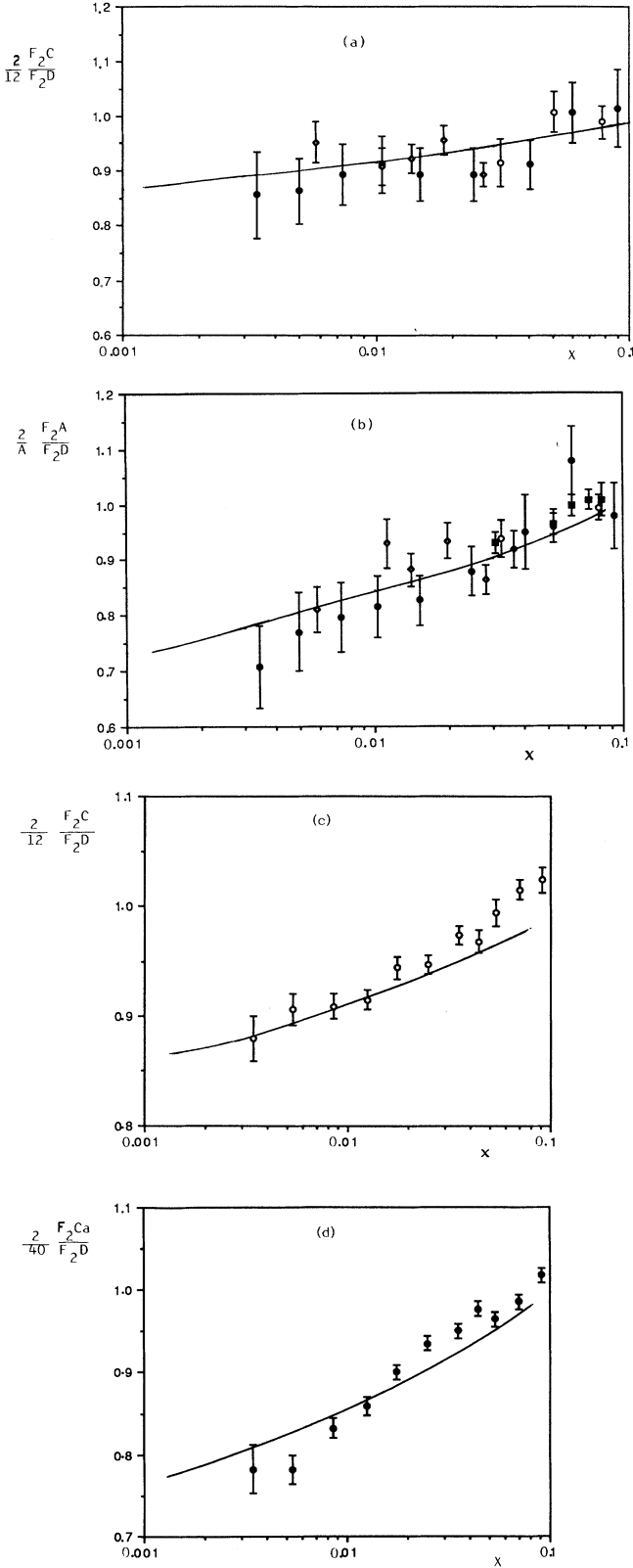


FIG. 13. Description of the data on $(2/A)(F_{2A}/F_{2D})$ for (a) $A = 12$ (data from Ref. [24]), (b) $A = 65$ (data from Refs. [24]), (c) $A = 12$ (data from Ref. [25]) and (d) $A = 40$ (data from Ref. [25]).

but for $E > E_M$ deviations from this dependence are present in Eq. (19).

To determine the constant g more precisely one can use experimental data on deep inelastic processes. The A dependence of nuclear structure functions is expressed as

$$F_{2A}(x_2) \propto \int d^2b \frac{n_A(b)}{1 + n_A(b)\tilde{C}(x_+) \exp[-(x_2/x_{2A}^{\text{crit}})^2]} \quad (20)$$

This formula determines the screening effects in the low- x_2 region. (A similar expression was found in Ref. [19].)

A comparison of the expression (20) for $g = 1$ mb with the available experimental data [24,25] on deep inelastic scattering on nuclei is shown in Fig. 13. The model reproduces the magnitude and x_2 dependence of the data (parton screening).

For the Drell-Yan process it follows from Eq. (19) that at present energies and masses $M \geq 5$ GeV the deviations from the A^1 dependence are very small, especially in the region of small x_F . Only at the highest available energy and for $x_F > 0.4$ there are small but measurable differences of α_{DY} from unity. It is shown in Fig. 14 that our prediction agrees with experimental data of the E772 Collaboration [11].

Consider now heavy-quark-state production. In this case Eq. (19) should be modified in order to take into account the " $Q\bar{Q}$ " interactions. We write, in this case,

$$f_{hA}^a(x_F, p_T^2) = f_{hN}^a(x_F, p_T^2) \times \int d^2b \frac{n_A(b)\mathcal{A}[\xi(x_+)\sigma_{Q\bar{Q}}n_A(b)]}{1 + n_A(b)\tilde{C}(x_+)\Phi} \quad (21)$$

The absorption factor \mathcal{A} (see the Appendix)

$$\mathcal{A}(z) = [1 - \exp(-z)]/z, \quad (22)$$

where $z = \xi(x_+)\sigma_{Q\bar{Q}}n_A(b)$, $\xi(x_+) = (1 - \epsilon) + \epsilon x_+^\gamma$, and $\sigma_{Q\bar{Q}}$, ϵ , and γ are some phenomenological parameters, which depend on the type of quark Q .

To describe J/ψ production on nuclei we use expres-

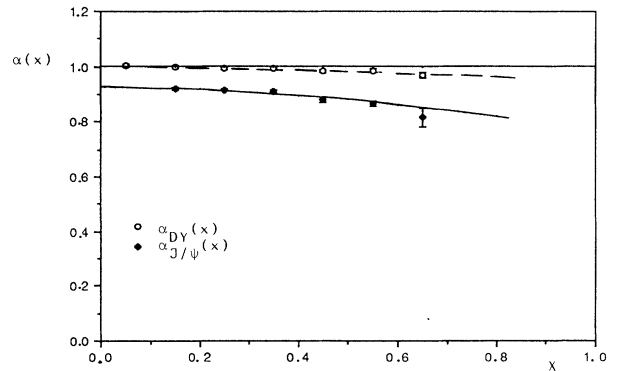


FIG. 14. Dependence on x of $\alpha(x)$ for Drell-Yan and J/ψ production at 800 GeV (data from Refs. [11]).

TABLE II. Comparison of the theoretical predictions on ψ photoproduction with experimental data [26]. $T_A = \sigma_{\gamma A \rightarrow \psi X} / A \sigma_{\gamma N \rightarrow \psi X}$.

	T_{Be}	T_{Fe}	T_{Pb}	$\frac{T_{Be}}{T_{Ta}}$
Expt	1.00 ± 0.50 [26(c)]	0.76 ± 0.05 [26(c)]	0.76 ± 0.08 [26(c)]	1.21 ± 0.08 [26(a)]
Theor	0.93	0.82	0.73	1.27

sions (21) and (22) with $\gamma=2$ (see the Appendix). The best values of the parameters for the description of the data on hadroproduction of J/ψ are

$$\epsilon = 0.75, \quad \sigma_{Q\bar{Q}} = 20 \text{ mb}. \quad (23)$$

Note that in the experiments on photo and electroproduction of J/ψ [26] an integration over x_F of J/ψ is performed, so the effect due to momentum conservation is not present and only the first term in the function $\xi(x_+)$ contributes. The experimental results on the A dependence of these reactions [26] are reproduced (see Table II).

The description of hadroproduction of J/ψ at different energies and for different nuclei are shown in Figs.

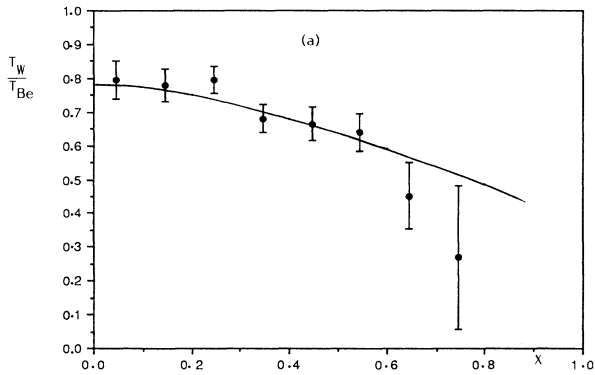


Fig 15a

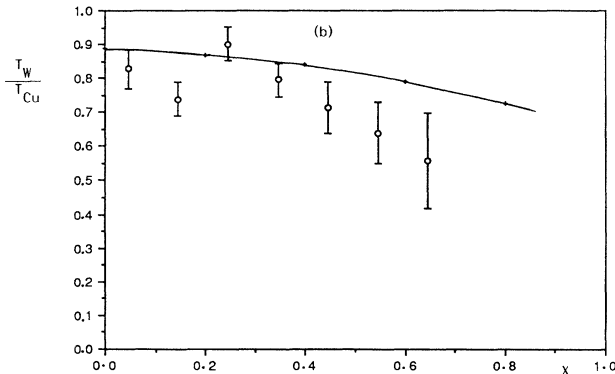


FIG. 15. Ratios of J/ψ -production cross section $T_A = (1/A)[\sigma(hA \rightarrow \psi X) / \sigma(hN \rightarrow \psi X)]$ in πA collisions at 125 GeV for (a) W/Be and (b) W/Cu (data from Ref. [12(e)]).

15–18, and the values of $\alpha(x_F)$ at 800 GeV are compared to the theoretical curve in Fig. 14. The description of the data is good in general. However, it is worth mentioning that the data of Refs. [12(d)] and [12(e)], measured in the same energy range, are not in complete agreement with each other, the points of Ref. [12(e)] (Fig. 15) showing more absorption than those of Ref. [12(d)] (Fig. 16).

The data of Ref. [11] at 800 GeV are in good agreement with our theoretical predictions and confirm the increase of absorption [decrease of $\alpha(x_F)$] with energy in the region of $x_F \approx 0.2-0.4$ predicted by our model. This change of absorption is due to the form factor Φ in Eq. (21) which varies with energy and this leads to small but observable effects. This effect is not very large because of the smallness of the coupling ($g = 1 \text{ mb}$).

Let us mention that the usual parametrization $f_{hA}^a \sim A^{\alpha(x_F)}$ is only approximate and the value of $\alpha(x_F)$ depends on the chosen range of nuclei. For example, if we consider only nuclei starting from C then the theoretical curve for $\alpha(x_F)$ in Fig. 14 will be 0.02–0.03 lower than the one determined in the same way as in the experiment, i.e., including the deuteron. A strong deviation from a straight-line dependence of T_A as a function of $\ln A$ is seen in the data of Ref. [12(e)]. Although the data of Ref. [11] can be described by a straight-line fit, they are better described by our theoretical curves, which have some curvature. Finally the data of Ref. [12(f)] show no deviation from the A^α law for $A > 12$. The model shows some small deviation which is consistent with the data (see Fig. 18). This possible change in the value of $\alpha(x_F)$, when different nuclei are used in the analysis, should be

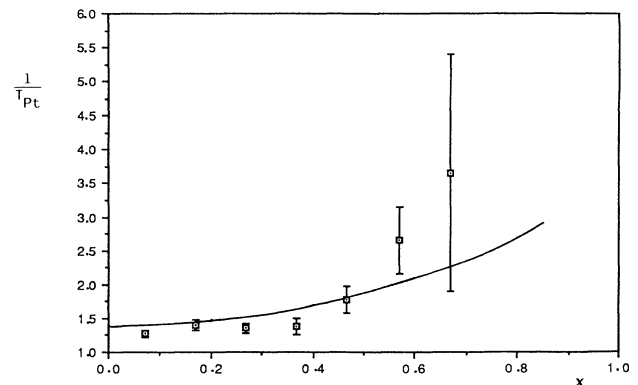


FIG. 16. The value of $1/T_A$ for pPt interactions at 200 GeV/c (data from Ref. [12(d)]).

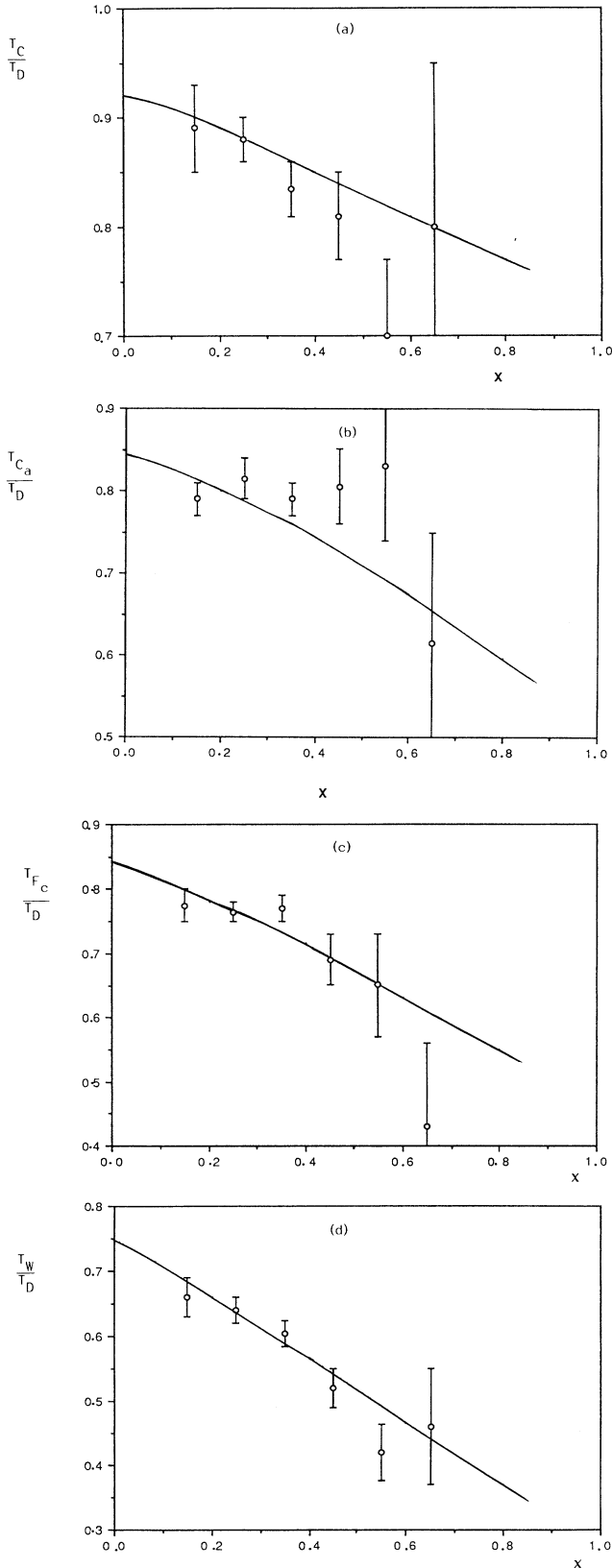


FIG. 17. The values of T_A/T_D in pA interactions at 800 GeV/c for (a) C/D, (b) Ca/D, (c) Fe/D, and (d) W/D (data from Refs. [11]).

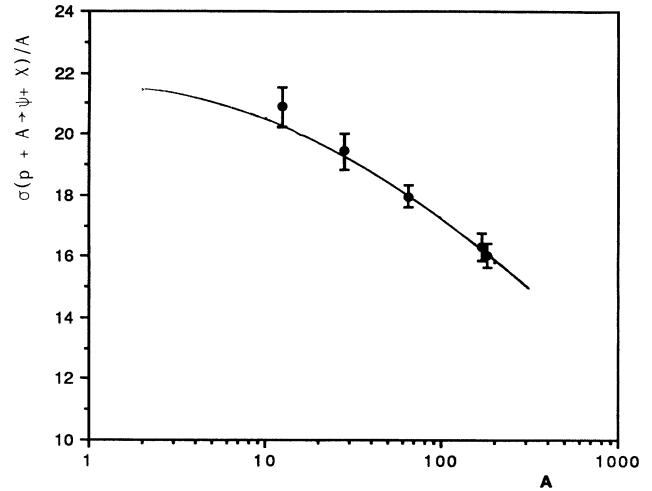


FIG. 18. $A^{-1}\sigma(pA \rightarrow \psi + X)$ vs A . (Data from Ref. [12(f)].)

taken into account when a comparison of $\alpha(x_F)$ from different experiments is made.

VII. COMPARISON WITH OTHER MODELS

Most of the present theoretical models for J/ψ production in hA and AA collisions [13] use some qualitative arguments, based on a semiclassical picture of hadronic interactions like “production” or “formation times.” These notions are often not very well defined and can sometimes be misleading. The difference between the cascade models with “formation time” and the Reggeon approach, based on the analysis of Feynman diagrams has been demonstrated in Ref. [8]. For J/ψ production, the models with “formation time” which increases proportionally to the energy of J/ψ , predict a decrease of the absorption effects as E_ψ increases, contrary to the experimental observations. The latter show that at a given energy absorption increases with x_F (and thus with E_ψ), and this increase starts at lower values of x_F as the initial energy increases. In Refs. [13(a),13(f)] an interaction with “comovers” was introduced. However, this interaction cannot explain the strong increase of absorption with x_F .

In Ref. [27(a)] an “intrinsic charm” component was proposed to explain the observed A dependence of J/ψ production on x_F . Interaction with “comovers,” final-state interaction with the “formation time” taken into account and shadowing in nuclear structure functions are also included in a recent quantitative description of experiment [27(b)]. It is assumed in this model that there is an “intrinsic charm” component in the initial hadron, which consists of a $c\bar{c}$ state and usual soft quarks and gluons. Strong interaction of these soft partons with nucleons leads to an $A^{2/3}$ behavior of J/ψ inclusive cross section in the region of $x_F \sim 1$, because J/ψ in this component carries a large part of the initial hadron energy.

In our approach the equivalent mechanism is the one described by the diagram of Fig. 9. We have shown that at $E < E_M$ this contribution is suppressed due to the t_{\min}

effect discussed in Sec. II. At $E > E_M$ this mechanism is not suppressed and for x not too close to one is essentially described by the enhanced diagram of Fig. 10. Because of the smallness of the triple-Pomeron coupling it does not lead to big effects. Note that this mechanism is just a shadowing of the nucleon structure function.

Our explanation of the decrease of $\alpha_\psi(x_F)$ with increasing x_F is based on a similar mechanism—except that the heavy-quark system (and not only the light quarks) participates in the interaction (i.e., there is rescattering of the heavy-quark system). In this sense such a mechanism combines features of both the intrinsic charm one and the comovers interaction. The mechanism is similar to the one for light hadrons: interactions of the $Q\bar{Q}$ pair taking into account energy-momentum conservation. Note that these effects do not decrease as the energy increases because for large energies, when the “formation time” is larger than the size of the nucleus, the fluctuation is prepared before it reaches the nucleus (see Sec. II).

Finally it is important to mention a recent discussion on new QCD production mechanisms for hard processes at x close to one [29]. It is shown in this paper that higher-twist subprocesses are not suppressed in the high x_F regime with $(1-x_F)Q^2$ fixed. In this regime the intrinsic charm mechanism of Ref. [27] may become dominant at large enough energies.

VIII. CONCLUSIONS

We have presented a unified picture of the production of hadrons made of either light or heavy quarks and of Drell-Yan pair production. The observed A dependence for all these processes can be qualitatively understood and the available experimental data are well described in a simple phenomenological model. The important role of a new high-energy scale, which arised for heavy particle production on nuclei, is emphasized.

It follows from our approach that there are rescattering effects, which can lead to violation of the factorization theorem of perturbative QCD. For heavy lepton-pair production the main ($3P$)-contribution is factorizable, while for heavy-quark production there is a big effect (especially for $x_F \rightarrow 1$), which leads to a violation of factorization.

Investigation of the properties of J/ψ (ψ', χ, \dots) production in hA collisions is important for understanding the mechanism of J/ψ suppression in nucleus-nucleus collisions.

The same method, based on the Glauber-Gribov approach, can be used also for these processes. Application of the model considered above to AB collisions is in progress. However, it can be anticipated that the results will be very close to those obtained in Ref. [13(e)].

Finally we summarize some of the predictions of our approach for future experiments.

(a) Cross sections for heavy-lepton production will deviate from an A^1 behavior with increasing energies. The characteristic energy scale is given by Eq. (3).

(b) The value of $\alpha_\psi(x_F)$ must gradually decrease as energy increases in the region of low x_F . At $x_F \sim 1$, $\alpha_\psi(x_F)$ is practically energy independent for $E \geq 100$ GeV.

(c) For $b\bar{b}$ states ($\Upsilon, \Upsilon', \dots$) $\alpha(x_F)$ should be practically x_F independent up to $x_F \approx 0.7-0.8$. At larger x_F it should decrease due to momentum-conservation effects.

(d) The decrease of $\alpha_\gamma(x_F)$ with energy starts at energies higher than the ones presently available. (See Table I.)

(e) The strength of the absorption at $x_F \approx 1$, and consequently the values of $\alpha(x_F \sim 1)$ should be approximately the same for different states made out of quarks of the same type (e.g., $\psi, \psi', \chi_j, D\bar{D}, \dots$).

All these predictions can be checked at future accelerators with nuclear beams, as the BNL Relativistic Heavy Ion Collider and CERN Large Hadron Collider.

ACKNOWLEDGMENTS

We would like to thank M. Braun, C. Pajares, Yu. Simonov, and K. Ter-Martirosyan for useful discussions. One of us (A.K.) is grateful to the Lab. de Phys. Theorique et Hautes Energies of Orsay for its hospitality. Laboratoire de Physique Théorique et Hautes Energies is Laboratoire Associé au CNRS.

APPENDIX

In this Appendix we describe the absorption model with a single dominant channel (“ $Q\bar{Q}$ ” state). After multiple scatterings this state eventually transforms into a given particle a plus hadrons.

Let the x_+ distribution of the “ $Q\bar{Q}$ ” system produced in hN interaction be $F_1^{Q\bar{Q}}(x_+)$. Moving through the nucleus the “ $Q\bar{Q}$ ” system can rescatter both elastically (not changing its momentum) and in elastically. In the latter case it can either lose some part of its momentum, or “disappear,” producing other heavy-quark states weakly coupled to particle a . We parametrize the probability to produce these states in a single rescattering by a parameter $(1-\epsilon)$. So for k inelastic scatterings the probability to remain a “ $Q\bar{Q}$ ” state is proportional to ϵ^k .

The change of the momentum under the rescattering can be characterized by some function $G^{Q\bar{Q}}$. Thus

$$F_{k+1}(x_+) = \epsilon \int_{x_+}^1 \frac{dx}{x} F_k(x) G^{Q\bar{Q}}(x_+/x). \quad (\text{A1})$$

We will denote this convolution as

$$F_{k+1} = \epsilon F_k \otimes G^{Q\bar{Q}}. \quad (\text{A2})$$

After production (and scatterings) the “ $Q\bar{Q}$ ” system transforms into the particle a and some hadrons. This stage can be characterized by a convolution with some new function $G^a(z)$:

$$F_k^a = F_k^{Q\bar{Q}} \otimes G^a. \quad (\text{A3})$$

It is important that the ordering of convolutions can be changed, so that

$$F_{k+1}^a = \epsilon^k F_1^{Q\bar{Q}} \otimes G^a \otimes G_k^{Q\bar{Q}}, \quad (\text{A4})$$

where $G_k^{Q\bar{Q}}$ is a k -fold convolution of $G^{Q\bar{Q}}$'s. As a result, we can use instead of two unknown functions $F_1^{Q\bar{Q}}$ and G^a

the function $F_1^a(x_+)$ which can be taken from experimental data on a spectra in hadron-nucleon.

Let us parameterize the functions $F_1^a(x_+)$ and $G^{Q\bar{Q}}(z)$ in the form

$$F_1^a(x_+) = C_a(1-x_+)^{n_a}, \quad G^{Q\bar{Q}}(z) = \beta_{Q\bar{Q}} z^{\beta_{Q\bar{Q}}}, \quad (\text{A5})$$

where the function $G^{Q\bar{Q}}(z)$ satisfies a normalization condition due to heavy-quark conservation:

$$\int_0^1 G^{Q\bar{Q}}(z) \frac{dz}{z} = 1.$$

The mean value of the momentum carried by the “ $Q\bar{Q}$ ” state after an inelastic collision is $\bar{z} = \beta_{Q\bar{Q}}(1 + \beta_{Q\bar{Q}})$. A simple estimate gives $\bar{z} = M_{Q\bar{Q}} / (M_{Q\bar{Q}} + \mu)$, where μ is some characteristic scale for light hadrons ($\mu \sim m_\rho$). Thus $\bar{z} \rightarrow 1$ and $\beta_{Q\bar{Q}}$ increases with an increase of $M_{Q\bar{Q}}$. It follows from Eqs. (A4) and (A5) that $F_{k+1}^a(0) = C_a \epsilon^k$. The difference between $F_k^a(x_+)$ and $F_{k+1}^a(x_+)$ is mainly concentrated in the region of x_+ close to unity. For $c\bar{c}$ states parameters of the function $F_1^a(x_+)$ can be determined from the data on J/ψ production in hN collisions [12]. The value of the parameter $\beta_{c\bar{c}}$ can be estimated from the data on the spectra of J/ψ in photo- and electroproduction [26]. This data show that J/ψ carries a substantial fraction of the initial momentum of the photon (i.e., of the $c\bar{c}$ pair into which the photon transforms) and $\beta_{c\bar{c}} \geq 6$.

To simplify the model we will use a simple parametrization of F_k^a in a form that reflects the softening of these functions as k increases and is consistent with the discussion above:

$$F_{k+1}^a(x_+) = F_1^a(x_+) \epsilon^k (1-x_+^\gamma)^k, \quad (\text{A6})$$

where γ is a parameter, which increases with the mass of the produced system. Numerical estimates, based on Eqs. (A4) and (A5) and the discussion that follows it, give $\gamma \approx 1.5-2.5$ for $c\bar{c}$ states and $\gamma \approx 4-5$ for $b\bar{b}$ systems.

We turn next to the expression of the cross sections σ_{k+1} involving one interaction in which the “ $Q\bar{Q}$ ” system is formed and k inelastic rescatterings of this system. These cross sections have a different form in the high-energy region $E > E_M$ and at low energies.

At energies $E < E_M$ the rescatterings are ordered in longitudinal direction and the cross sections are

$$\sigma_{k+1} = \int d^2b \int_0^{n_A(b)} \sigma_{hN}^a dv \frac{(\sigma_{Q\bar{Q}} v)^k}{k!} \exp(-\sigma_{Q\bar{Q}} v). \quad (\text{A7})$$

Thus at these energies the absorption is determined by the formula

$$\begin{aligned} f_{hA}^a(x_+) &= \sum_{k=1}^{\infty} \sigma_k F_k^a(x_+) \\ &= f_{hN}^a(x_+) \int d^2d \int_0^{n_A} dv \exp[-\xi(x_+) \sigma_{Q\bar{Q}} v] \\ &= f_{hN}^a(x_+) \int d^2b \frac{1 - \exp[-\xi(x_+) \sigma_{Q\bar{Q}} n_A(b)]}{\xi(x_+) \sigma_{Q\bar{Q}}}, \end{aligned} \quad (\text{A8})$$

where the function $f_{hN}^a(x_+) = \sigma_{hA}^a F_1^a(x_+)$ and $\xi(x_+) = (1-\epsilon) + \epsilon x_+^\gamma$ determines the x_+ dependence of the strength of the shadowing. With $\xi(x_+) = 1$ one recovers the well-known Glauber formula with longitudinal ordering (cf. Eq. (1) of Ref. [13(c)]). We recover in this way the absorption factor $\mathcal{A}(z)$ in Eqs. (22).

At high energies $E > E_M$, t_{\min} effects are not important and, as a result, Eqs. (A7) and (A8) are modified. Furthermore, coherent diffractive production of heavy states becomes possible. When both effects are taken into account the transition between the two energy regions is rather smooth. In particular, for $x_+ \sim 1$ the absorption factor coincides with the low-energy one [Eq. (A8)] to lowest order. For this reason, and also for simplicity, we use Eq. (A8) in the whole energy region.

-
- [1] V. N. Gribov, in Proceedings of the VII LIYF Winter School of Physics, Leningrad, USSR, 1973, Vol. 11, p. 5; V. N. Gribov, Zh. Eksp. Teor. Fiz. **53**, 654 (1967) [Sov. Phys. JETP **26**, 414 (1968)].
- [2] R. J. Glauber, in *Lectures in Theoretical Physics*, edited by W. E. Britten (Interscience, New York, 1959), Vol. 1, p. 315; A. G. Sitenko, Ukr. Phys. J. **4**, 152 (1959).
- [3] V. N. Gribov, Zh. Eksp. Teor. Fiz. **56**, 892 (1969) [Sov. Phys. JETP **29**, 483 (1969)]; **57**, 1306 (1969) [**30**, 709 (1970)].
- [4] A. Capella *et al.*, Z. Phys. C **3**, 329 (1980); A. Capella and J. Tran Thanh Van, Phys. Lett. **114B**, 450 (1982); Z. Phys. C **10**, 249 (1981).
- [5] A. B. Kaidalov, Phys. Lett. **116B**, 459 (1982); A. B. Kaidalov and K. A. Ter-Martirosyan, *ibid.* **117B**, 247 (1982); A. B. Kaidalov, K. A. Ter-Martirosyan, and Yu. M. Shabelski, Yad. Fiz. **43**, 1282 (1986) [Sov. J. Nucl. Phys. **43**, 822 (1986)].
- [6] V. Abramovsky, V. N. Gribov, and O. V. Kancheli, Yad. Fiz. **18**, 595 (1973) [Sov. J. Nucl. Phys. **18**, 308 (1974)].
- [7] A. Capella and A. Kaidalov, Nucl. Phys. **B111**, 477 (1976); A. Capella and A. Kryzwicki, Phys. Rev. D **18**, 3357 (1978).
- [8] K. G. Boreskov, A. B. Kaidalov, S. M. Kiselev, and N. Ya. Smorodinskaya, Yad. Fiz. **53**, 569 (1991) [Sov. J. Nucl. Phys. **53**, 356 (1991)].
- [9] K. G. Boreskov and A. B. Kaidalov, in *High Energy Hadronic Interactions '91*, Proceedings of the XXVth Rencontre de Moriond, Les Arcs, France, edited by J. Tran Thanh Van (Editions Frontières, Gif-sur-Yvette, 1991).
- [10] W. N. Geist, in *Quark Matter 90*, Proceedings of the Conference, Menton, France, edited by J. P. Blaizot *et al.* [Nucl. Phys. **A525**, 149c (1991)].
- [11] D. M. Alde *et al.*, Phys. Rev. Lett. **66**, 133 (1991); C. S. Mishra *et al.*, in *High Energy Hadronic Interactions*, Proceedings of the 25th Rencontre de Moriond, Les Arcs, France, 1990, edited by J. Tran Thanh Van (Editions Frontières, Gif-sur-Yvette, 1990), p. 255.
- [12] (a) J. G. Branson *et al.*, Phys. Rev. Lett. **38**, 1334 (1977);

- (b) Yu. M. Antipov *et al.*, Phys. Lett. **76B**, 235 (1978); (c) M. J. Corden *et al.*, *ibid.* **110B**, 415 (1982); (d) J. Badier *et al.*, Z. Phys. C **20**, 101 (1983); (e) S. Katzanavas *et al.*, Phys. Rev. Lett. **60**, 2121 (1988); (f) NA38 Collaboration, L. Fredj, Ph.D. thesis, University of Clermond-Ferrand (France).
- [13] (a) S. J. Brodsky and A. H. Mueller, Phys. Lett. **206**, 685 (1988); (b) S. Gavin, M. Gyulassy, and A. Jackson, *ibid.* **207**, 257 (1988); (c) A. Capella *et al.*, *ibid.* **206**, 354 (1988); (d) J. P. Blaizot and J. Y. Ollitrault, *ibid.* **217**, 386 (1989); (e) A. Capella *et al.*, *ibid.* **243**, 144 (1990); in *High Energy Hadronic Interactions* [11]; (f) S. Gavin and R. Vogt, Nucl. Phys. **B345**, 104 (1990); (g) G. Gerschel and J. Hüfner, Phys. Lett. **B 207**, 253 (1988).
- [14] S. Mandelstam, Nuovo Cimento **30**, 1113 (1963); **30**, 1127 (1963); **30**, 1148 (1963).
- [15] M. A. Braun, Yad. Fiz. **47**, 262 (1988) [Sov. J. Nucl. Phys. **47**, 164 (1988)]; **52**, 257 (1990) [Sov. J. Nucl. Phys. **52**, 164 (1990)].
- [16] G. T. Bodwin *et al.*, Phys. Rev. Lett. **47**, 1799 (1981).
- [17] L. Frankfurt and M. Strikman, Phys. Rep. **160**, 235 (1988).
- [18] N. N. Nikolaev and V. I. Zakharov, Phys. Lett. **55B**, 397 (1975); E. M. Levin and M. G. Ryskin, Yad. Fiz. **41**, 472 (1985) [Sov. J. Nucl. Phys. **41**, 300 (1985)]; A. H. Mueller and J. Qiu, Nucl. Phys. **B268**, 427 (1986); E. L. Berger and J. Qiu, Phys. Lett. **B 206**, 41 (1988); F. E. Close and R. G. Roberts, *ibid.* **213**, 91 (1988).
- [19] J. Kwiecinski and B. Badelek, Phys. Lett. **B 208**, 508 (1988); J. Kwiecinski, Z. Phys. C **45**, 461 (1989).
- [20] G. T. Bodwin, Phys. Rev. D **31**, 2616 (1985).
- [21] A. Schwimmer, Nucl. Phys. **B94**, 445 (1975); J. C. Collins, D. E. Soper, and G. Sterman, *ibid.* **B261**, 104 (1985); **B308**, 833 (1988).
- [22] A. B. Kaidalov, Phys. Rep. **50**, 157 (1979).
- [23] M. A. Preston and R. K. Bhaduri, *Structure of the Nucleus* (Addison-Wesley, New York, 1975).
- [24] J. Eickmeyer *et al.*, Phys. Rev. Lett. **36**, 289 (1976); S. Stein *et al.*, Phys. Rev. D **12**, 1884 (1975); EMC, A. Anedo *et al.*, Phys. Lett. **B 211**, 493 (1988); EMC, J. Ashman *et al.*, *ibid.* **202**, 603 (1988).
- [25] New Muon Collaboration, P. Amaudruz *et al.*, Z. Phys. C **51**, 387 (1991).
- [26] (a) R. L. Anderson *et al.*, Phys. Rev. Lett. **38**, 263 (1977); (b) J. J. Aubert *et al.*, Phys. Lett. **89B**, 267 (1980); **152B**, 433 (1985); Nucl. Phys. **B213**, 1 (1983); (c) M. D. Sokoloff *et al.*, Phys. Rev. Lett. **57**, 3003 (1986).
- [27] (a) S. J. Brodsky and P. Hoyer, Phys. Rev. Lett. **63**, 1566 (1989); (b) R. Vogt, S. J. Brodsky, and P. Hoyer, Nucl. Phys. **B360**, 67 (1991).
- [28] H. E. Miettinen and P. M. Stevenson, Phys. Lett. **B 199**, 591 (1987). For a somewhat different approach see Ref. [27(a)].
- [29] S. J. Brodsky, P. Hoyer, A. H. Muller, and W. K. Tang, Nucl. Phys. **B369**, 519 (1992).